Resonant and Near-Threshold Photoionization Cross Sections of Fe^{14+}

M. C. Simon,[1,*] J. R. Crespo López-Urrutia,[1,†] C. Beilmann,[1] M. Schwarz,[1] Z. Harman,[1,2] S. W. Epp,[1] B. L. Schmitt,[1] T. M. Baumann,[1] E. Behar,[3] S. Bernitt,[1] R. Follath,[4] R. Ginzel,[1] C. H. Keitel,[1] R. Klawitter,[1] K. Kubiček,[1] V. Mäckel,[1] P. H. Mokler,[1] G. Reichardt,[4] O. Schwarzkopf,[4] and J. Ullrich[1]

[1]*Max-Planck-Institut für Kernphysik, Saupfercheckweg 1, 69117 Heidelberg, Germany*
[2]*ExtreMe Matter Institute EMMI, Planckstrasse 1, 64291 Darmstadt, Germany*
[3]*Physics Department, Technion Israel Institute of Technology, Haifa 32000, Israel*
[4]*Helmholtz–Zentrum Berlin, BESSY II, Albert-Einstein-Straße 15, 12489 Berlin, Germany*

(Received 20 March 2009; revised manuscript received 5 November 2009; published 27 October 2010)

Photoionization (PI) of Fe^{14+} in the range from 450 to 1100 eV was measured at the BESSY II storage ring using an electron beam ion trap achieving high target-ion area densities of 10^{10} cm^{-2}. Photoabsorption by this ion is observed in astrophysical spectra and plasmas, but until now cross sections and resonance energies could only be provided by calculations. We reach a resolving power $E/\Delta E$ of at least 6500, outstanding in the present energy range, which enables benchmarking and improving the most advanced theories for PI of ions in high charge states.

DOI: 10.1103/PhysRevLett.105.183001 PACS numbers: 32.80.Fb, 37.10.Ty, 95.30.Dr

Understanding the photoionization (PI) of highly charged ions (HCIs) is a premise for the interpretation of astrophysical observations of accretion sources such as active galaxies (quasars) and x-ray binaries photoionizing their ambient gas. The study of these sources is largely based on the observation of PI and spectral-line absorption. According to cosmological models, roughly half of all baryons in the Universe constitute the warm-hot intergalactic medium (WHIM) [1], of which the coolest part has been detected by means of UV absorption of O^{5+} [2]. It is a subject of current debate whether PI is the dominant ionization process in the WHIM [3]. PI by background radiation has recently been shown to totally change astrophysical cooling estimates [4]. Certainly, HCI opacities also play an important role in the solar model, since the interpretation of helioseismology data [5] and the estimation of element abundances rely heavily on the photoabsorption cross sections assumed in the radiation transport equations.

Reliably calibrated data on PI of HCI are scarce (cf. [6,7]), and astrophysical models, for the most part, use computed cross sections and rates. Since astrophysical absorbers are often in motion, it is impossible to disentangle line energies from kinematic (Doppler) uncertainties. Recently, apparent differences in measured outflow velocities in the active galaxy NGC 3783 were first ascribed to two kinematic components [8], a conclusion that was later put into doubt on the basis of improved atomic calculations [9]. Laboratory PI measurements as presented in this work for Fe^{14+} are thus crucial for benchmarking competing theoretical approximations. This need is especially urgent for M-shell ions of Fe, such as Fe^{14+} that produce conspicuous unresolved transition arrays in x-ray spectra [10,11]. Such signatures are also found in spectra from laser-produced and fusion plasmas, e.g., in tokamaks, where Fe impurities contribute significantly to radiative cooling, and constitute an important diagnostic tool.

PI measurements to date have not included ions in charge states as high as $q = 14$ and photon energies around 1 keV at the level of accuracy presented here. Besides dual-plasma methods utilizing separate plasmas for the radiation source (either laser produced or Z pinch) [6,12–16] and for the absorbing medium, the merged beam technique has been employed; see, e.g., [6,7]. In that method, a tenuous ion beam of typical area densities below 10^7 cm^{-2} is merged with a photon beam from a synchrotron source, and the photoion yield is detected. So far its application has been limited to ions with an ionization potential $E_{\mathrm{IP}} \lesssim 150$ eV [17,18]. Significantly higher photon energies have been applied only for subshell excitations on ions in low charge states such as C^{2+} [19]. Moreover, just two PI measurements using trapped ions have been reported until now, both in Penning traps at typical target densities of 10^6 cm^{-2}. There, Ar^{2+} ions were exposed to broadband synchrotron radiation producing K-shell vacancies [20]. Photoions up to Ar^{8+} resulted from the subsequent electron shakeoff. Recently, Xe^+ was photoionized [21], and the Fourier transform ion-cyclotron resonance method was applied to detect Xe^{2+} photoions.

In this Letter, we present experimental PI data for the astrophysically relevant Mg-like Fe^{14+} ion from threshold up to the keV range. The ions are produced and stored in an electron beam ion trap (EBIT) and subsequently photoionized by synchrotron radiation. We measured PI resonance excitation energies with an accuracy of 150 meV at 800 eV (mainly calibration limited). This method gives access to ions in higher charge states than previously investigated by other techniques, exploiting its high target-ion area density of 10^{10} cm^{-2}, while combining the charge-state selectivity of an EBIT and the excellent

spectral resolution of synchrotron monochromators. Additionally, the feasibility of measuring resonance strengths and, hence, also of determining cross sections is demonstrated. A similar scheme was proposed [22] and tested using an electron beam ion source [23–25], but no PI results for HCIs have been reported so far.

The experiment was performed at the monochromator beam line U49/2-PGM1 [26] of the BESSY II storage ring with the transportable FLASH-EBIT [27]. The experimental scheme is displayed in Fig. 1. At the trap center of the EBIT, ions are produced through electron impact ionization (EII) by an electron beam and confined radially by its negative space charge. This beam is emitted from a cathode at a potential U_{cath}, accelerated toward an assembly of drift tubes, compressed to 50 μm diameter by a magnetic field of 6 T, and dumped on a collector. Voltages applied to the drift tubes configure a thin cylindrical trapping volume (diameter $\lesssim 250$ μm, length 50 mm). The ions are exposed to the photon beam, which is brought to axial overlap. It is crucial to keep the electron beam energy E^e_{kin} below the ionization potential E_{IP} of the PI process under investigation since otherwise EII would completely dominate over PI. To detect PI, both the target ions and the up-charged ions (mostly photoions) were ejected from the trap, guided through the annular collector, and electrostatically deflected off the photon beam axis. After charge analysis by a Wien filter, they were simultaneously counted on a two-dimensional position sensitive detector, where they impinge upon separate regions due to their different charge-over-mass values (q/m). Their yield ratio was normalized to the photon flux and recorded as a function of the photon energy selected by the monochromator and calibrated by photoabsorption lines of neutral N_2 (at 400 eV) and Ne (at 860 eV) with an accuracy of 100 meV limited by the uncertainties of these lines.

The PI signal can be converted to a resonance strength or to a cross section scale according to Kravis *et al.* [25], which we demonstrate below for the $2p_{1/2} - 3d_{3/2}$ resonance. This method relies on rate equations only sensitive to the time dependence of yield ratios for the extracted ions (independent of the absolute transport efficiency) and is enabled by the long trapping times possible in the EBIT. We determine the overlap of the photon beam and the ion cloud by moving into the trap center a retractable crystal capable of scintillating with electrons and photons (for further details, see [28,29]). As pointed out in [25], corrections for the effective overlap will not be needed when the narrow ion cloud is homogeneously illuminated by the photon beam, since the ion density drops out of the rate equations in that case.

In order to determine a value for PI, Fe^{14+} ions were confined in a deep trap (65 V) and continuously irradiated with a broadband photon beam ($\Delta E = 690$ meV), completely covering the $2p_{1/2} - 3d_{3/2}$ resonance at 807.1 eV. The electron beam remained on guaranteeing the highest possible ion density. During a measuring cycle the trap was emptied after well-defined time intervals varying from 1 to 10 s and the ion inventory was analyzed. In Fig. 2, a growing number of Fe^{15+} up-charged ions can be seen to build up with time, both with and without the photon beam. In accordance with the rate equations [25], the increase of the ion yield flattens at longer times due to the competing recombination processes, primarily, electron capture, and, to a lesser extent, charge exchange. The ionization without photons is caused by EII of long-lived metastable states $(Fe^{14+})^*$ $3s3p\,^3P_{0,1,2}$. With an excitation energy of ≈ 30 eV the population of these states through electron-ion collisions is unavoidable. At the present electron density ($\approx 10^{11}$ cm^{-3}) only $3s3p\,^3P_2$ should appear in significant abundances (below 10% of that of the GS [30]). Reducing the electron energy sufficiently to forestall Fe^{15+} production from that level would have compromised the Fe^{14+} production by bringing it too close to the $E^{\mathrm{Fe13+}}_{\mathrm{IP}} = 390$ eV threshold.

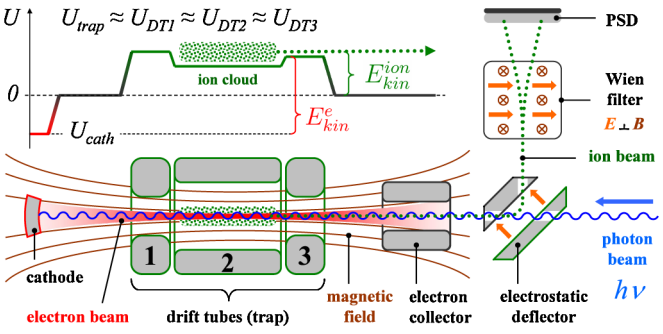

FIG. 1 (color online). Setup for PI measurements using synchrotron radiation and an EBIT equipped with ion extraction. HCIs produced and trapped by a compressed electron beam form a cloud with an area density of $\approx 10^{10}$ m^{-2} (e.g., Fe^{14+}) for axial overlap with a synchrotron beam. Both target ions and photoions are extracted, charge selected, and counted with a position sensitive detector (PSD).

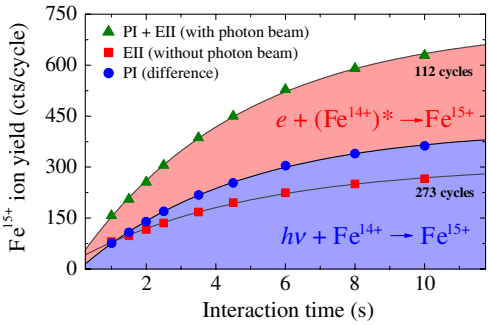

FIG. 2 (color online). Yield of Fe^{15+} ions versus interaction time with (green triangles) and without (red squares) photon beam. The difference of both curves gives the PI yield (blue dots). The red area above represents the EII yield from metastable $(Fe^{14+})^*$ ions. (273 and 112 measuring cycles were added with and without photon beam, respectively.)

The normalization run had to be carried out in the single-bunch synchrotron mode, at a low photon flux with a large inaccuracy in calibration (dating back to 2005). This, and an increased background due to the q/m coincidence of the target ion Fe^{14+} with O^{4+} and C^{3+}, resulted in a large uncertainty for the final value. We obtain for the $2p_{1/2} - 3d_{3/2}$ resonance a PI strength of (110 ± 60) Mbarn eV [see single point with error bars in Fig. 3(d); a precise recalibration of the photon flux will improve the experimental accuracy]. The result is in accordance with the theoretical values of 153, 129, and 141 Mbarn eV from HULLAC code version 1996 [31], large-scale multiconfiguration Dirac-Fock calculations (MCDF) [28], and relativistic many-body perturbation theory (RMBPT) [9], respectively.

The spectra, cf. Fig. 3, measured in multibunch mode with a well-monochromatized photon beam can be normalized by comparing the area under the resonance in Fig. 3(d) to the above determined experimental strength. Deconvoluting the 130 meV broad line by fitting a Voigt profile results in a Lorentz width of 105 meV, composed of the natural line width and an underlying spectrometer contribution. The natural line width which has to be compared to theoretical predictions of 36 meV (RMBPT), 86 meV (HULLAC), and 34 meV (MCDF) allows us to determine the cross section at the resonance. As in general line widths are smaller than the experimental resolution, resonance strengths are measured rather than cross sections. The scale can be cross-checked by normalizing an ionization edge to the theoretical cross section for direct PI. For the $3s$ edge, different calculations consistently predict a value of 136 kbarn. Being sensitive well below this level, as seen in Fig. 3(e), and assuming the theoretical PI cross section at the edge yields a resonance strength of (74 ± 36) Mbarn eV for the $2p_{1/2} - 3d_{3/2}$ line, in consistency with the value deduced via rate equations.

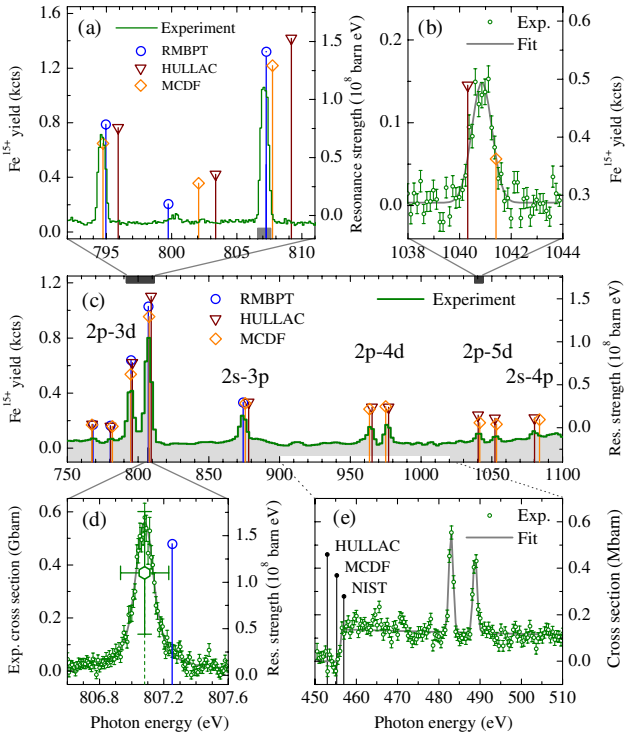

FIG. 3 (color online). Photoionization spectra for Fe^{14+} (detected by the Fe^{15+} yield). Peaks are due to autoionizing states resonantly excited by the photon beam. Experiment (Fe^{15+} yield, cross section), green step curve or circles, fits: gray line, theories (resonance strength): RMBPT Gu *et al.* [9]: blue circles; HULLAC and MCDF both this work: brown triangles and orange diamonds, respectively. (c) overview; (a), (b), and (d) details; (e) ionization edge and second-order photon peaks.

The threshold is found at 456.2(5) eV representing the first direct E_{IP} threshold measurement of an ion beyond $q = 9$ using PI. Predictions by HULLAC [31] and MCDF [28] both lie at lower values of 453.0 and 455.3 eV, respectively. The value compiled at the NIST database [32] of 457.0057 eV is found to be above the measurement.

In Fig. 3(c) an overview spectrum of PI of Fe^{14+} is shown in the range from 750 to 1100 eV. The main features are autoionizing photon-excited resonances, which include L-shell excitations. The $2p_{3/2} - 5d_{5/2}$ resonance at 1040.9(4) eV displayed in Fig. 3(b) is the last one resolved in detail. The two features at 482.3(2) and 488.0 (2) eV seen in Fig. 3(e) are caused by second-order diffracted photons exciting the $2p_{3/2} - 4d_{5/2}$ and $2p_{1/2} - 4d_{3/2}$ resonances found in first order at 964.3(2) and 975.8 (2) eV, respectively. Calculations from this work (HULLAC and MCDF) and by Gu *et al.* [9], who presented improved atomic data, at least for the strongest resonances based on second-order RMBPT, are shown as vertical lines giving their theoretical resonance strengths.

The achieved (calibration-limited) absolute photon energy accuracy suffices easily to distinguish and benchmark advanced calculations as shown by the detailed scan from 791 to 811 eV in Fig. 3(a). The strong resonances belong to the single electron transitions $2p_{3/2} - 3d_{5/2}$ at 794.7(2) eV and $2p_{1/2} - 3d_{3/2}$ at 807.1(2) eV. Predictions by HULLAC lie on average 1.3 eV above experimental resonances, or 26 mÅ at 16 Å as reported by Gu *et al.* [9]. This translates to Doppler shift uncertainties in emitter or absorber velocities of around 500 km/s, which are comparable to the velocity range of most outflows from active galaxies and x-ray binaries. R-matrix calculations show even larger deviations [33–35]. The agreement with the RMBPT calculations is quite satisfactory assuming a calibration error of 0.15 eV, and one can conclude that those are the best currently available, followed by MCDF values. However, for weaker resonances which include two-electron one-photon transitions [e.g., $2p_{1/2}3s_{1/2} - 3p_{1/2}3p_{3/2}$ at 800.3(2) eV] larger deviations appear for all theories. Table I lists experimental threshold and resonance energies from Figs. 3(a), 3(b), and 3(e) as well as deviations of different calculations ($E_{theo} - E_{expt}$).

TABLE I. Experimental PI edge E_{IP} and resonance energies compared with HULLAC (A) and MCDF (B) predictions from this work, and with available RMBPT (C) values [9] and R-matrix (D) results of Bautista [35]. Experimental results and theory deviations, $E_{theo} - E_{expt}$, are given in eV.

Transition	Expt.	A	B	C	D
E_{IP}: $3s_{1/2} - \infty$	456.2(5)	−3.2	−0.9	⋯	10.0
$2p_{3/2} - 3d_{5/2}$	794.7(2)	1.2	0.0	0.2	15.1
$2p_{1/2}3s_{1/2} - 3p_{1/2}3p_{3/2}$	800.3(2)	3.1	1.8	−0.6	⋯
$2p_{1/2} - 3d_{3/2}$	807.1(2)	2.1	0.6	0.2	⋯
$2p_{3/2} - 5d_{5/2}$	1040.9(5)	−0.6	0.5	⋯	19.5

Furthermore, the splitting of the two strong $2p - 3d$ resonances around 800 eV can be determined with remarkable accuracy to be 12.481(9) eV (HULLAC: 13.298 eV; MCDF: 13.005 eV; RMBPT: 12.303 eV). Also, by applying the theoretical value of 36 meV [9] for the natural line width to the detailed measurement on the $2p_{1/2} - 3d_{3/2}$ resonance displayed in Fig. 3(d), a resolving power of $E/\Delta E \approx 6500$ is achieved, outstanding for this energy range. One can deduce from the narrow line of the resonance that calibration improvements will enable even more stringent tests of theory. Using the PI ionization edge of H-like ions or accurately calculable resonances of He-like ions for this purpose could yield far more accurate standards than the ones currently available.

In summary, PI of Fe^{14+} with an ionization potential of 456.2 eV was directly observed and investigated using synchrotron radiation and an EBIT generating a high target area density of approximately 10^{10} cm^{-2}. The current energy resolution of our data benchmarks advanced calculations and confirms, e.g., a recent prediction for a single outflow component in the active galaxy NGC 3783 [9] which stands in contradiction with models based on inaccurate electronic structure predictions [8]. The strength of a strong resonance was determined from time-dependent measurements and cross-checked by comparison to theoretical direct PI cross section at the ionization threshold, where an experimental sensitivity in the tens of kbarn range was achieved.

More brilliant x-ray beams from synchrotrons such as PETRA III will allow us in the future to test relativistic and QED contributions to HCIs with even higher accuracy. Interesting insights into electronic correlations can be expected from PI investigations of long isoelectronic and isonuclear sequences. X-ray free-electron lasers, such as LCLS, will carry the study of photonic interactions into the relativistic regime, extend resonant laser spectroscopy in the multi-keV region, and allow for multiphoton excitation as well as for femtosecond pump-and-probe lifetime investigations with HCIs.

We thank K. Bechberger, N. Müller, T. Schiffmann, and S. Vogel of MPI-K, who deserve our special gratitude for their help. Supported by Helmholtz Alliance HA216/EMMI. B. L. S. is supported by a Fulbright grant.

*m.simon@mpi-hd.mpg.de
†crespojr@mpi-hd.mpg.de

[1] R. Cen and J. P. Ostriker, Astrophys. J. **514**, 1 (1999).
[2] B. D. Savage *et al.*, Astrophys. J. **564**, 631 (2002).
[3] F. Nicastro *et al.*, Astrophys. J. **629**, 700 (2005).
[4] R. P. C. Wiersma, J. Schaye, and B. D. Smith, Mon. Not. R. Astron. Soc. **393**, 99 (2009).
[5] S. Basu and H. Antia, Phys. Rep. **457**, 217 (2008).
[6] J. B. West, J. Phys. B **34**, R45 (2001).
[7] H. Kjeldsen, J. Phys. B **39**, R325 (2006).
[8] T. Holczer, E. Behar, and S. Kaspi, Astrophys. J. **632**, 788 (2005).
[9] M. F. Gu *et al.*, Astrophys. J. **641**, 1227 (2006).
[10] M. Sako *et al.*, Astron. Astrophys. **365**, L168 (2001).
[11] E. Behar, M. Sako, and S. M. Kahn, Astrophys. J. **563**, 497 (2001).
[12] G. Winhart *et al.*, Phys. Rev. E **53**, R1332 (1996).
[13] B. A. Remington, R. P. Drake, and D. D. Ryutov, Rev. Mod. Phys. **78**, 755 (2006).
[14] M. E. Foord *et al.*, Phys. Rev. Lett. **93**, 055002 (2004).
[15] J. E. Bailey *et al.*, Phys. Rev. Lett. **99**, 265002 (2007).
[16] R. F. Heeter *et al.*, Phys. Rev. Lett. **99**, 195001 (2007).
[17] J.-M. Bizau *et al.*, Phys. Rev. Lett. **84**, 435 (2000).
[18] A. Aguilar *et al.*, Phys. Rev. A **73**, 032717 (2006).
[19] S. W. J. Scully *et al.*, J. Phys. B **38**, 1967 (2005).
[20] S. D. Kravis *et al.*, Phys. Rev. Lett. **66**, 2956 (1991).
[21] R. Thissen *et al.*, Phys. Rev. Lett. **100**, 223001 (2008).
[22] D. A. Church *et al.*, J. Phys. B **17**, L401 (1984).
[23] S. D. Kravis *et al.*, Rev. Sci. Instrum. **65**, 1066 (1994).
[24] M. Oura *et al.*, Nucl. Instrum. Methods Phys. Res., Sect. B **86**, 190 (1994).
[25] S. D. Kravis *et al.*, Phys. Scr. **T71**, 121 (1997).
[26] K. Sawhney, F. Senf, and W. Gudat, Nucl. Instrum. Methods Phys. Res., Sect. A **467–468**, 466 (2001).
[27] S. W. Epp *et al.*, Phys. Rev. Lett. **98**, 183001 (2007).
[28] M. C. Simon *et al.*, J. Phys. B **43**, 065003 (2010).
[29] M. C. Simon *et al.*, J. Phys. Conf. Ser. **194**, 012009 (2009).
[30] S. O. Kastner and A. K. Bhatia, Astrophys. J. **553**, 421 (2001).
[31] A. Bar-Shalom, M. Klapisch, and J. Oreg, J. Quant. Spectrosc. Radiat. Transfer **71**, 169 (2001).
[32] Yu. Ralchenko, A. E. Kramida, J. Reader, and NIST ASD Team, NIST Atomic Spectra Database (version 3.1.5).
[33] K. Butler, C. Mendoza, and C. J. Zeippen, J. Phys. B **26**, 4409 (1993).
[34] N. Haque and A. K. Pradhan, Phys. Rev. A **60**, R4221 (1999).
[35] M. A. Bautista, J. Phys. B **33**, L419 (2000).